HHS Public Access

Author manuscript

Inhal Toxicol. Author manuscript; available in PMC 2017 October 01.

Published in final edited form as:

Inhal Toxicol. 2016 October ; 28(12): 550–560. doi:10.1080/08958378.2016.1226449.

Pulmonary distribution of nanoceria: comparison of intratracheal, microspray instillation and dry powder insufflation

Ramon M. Molina[*], **Nagarjun V. Konduru**, **Hugo Hirano**, **Thomas C. Donaghey**, **Benoit Adamo**[†], **Brendan Laurenzi**[†], **Georgios Pyrgiotakis**, and **Joseph D. Brain**

Molecular and Integrative Physiological Sciences Program, Department of Environmental Health, Harvard T.H. Chan School of Public Health, 665 Huntington Avenue, Boston, MA 02115, USA

[†]MannKind Corporation, 1 Casper St, Danbury, CT 06810

Abstract

Particles can be delivered to the respiratory tract of animals using various techniques. Inhalation mimics environmental exposure but requires large amounts of aerosolized NPs over a prolonged dosing time, varies in deposited dose among individual animals, and results in nasopharyngeal and fur particle deposition. Although less physiological, intratracheal (IT) instillation allows quick and precise dosing. Insufflation delivers particles in their dry form as an aerosol. We compared the distribution of neutron-activated $^{141}CeO_2$ nanoparticles (5 mg/kg) in rats after 1) IT instillation, 2) left intrabronchial instillation, 3) microspraying of nanoceria suspension, and 4) insufflation of nanoceria dry powder. Blood, tracheobronchial lymph nodes, liver, gastrointestinal tract, feces and urine were collected at 5 minutes and 24 hours post-dosing. Excised lungs from each rat were dried at room temperature while inflated at a constant 30 cm water pressure. Dried lungs were then sliced into 50 pieces. The radioactivity of each lung piece and other organs was measured. The evenness index (El) of each lung piece was calculated [$EI=(\mu Ci/mg_{piece})/(\mu Ci/mg_{lung})$]. The degree of EI value departure from 1.0 is a measure of deposition heterogeneity. We showed that the pulmonary distribution of nanoceria differs among modes of administration. Dosing by IT or microspraying resulted in similar spatial distribution. Insufflation resulted in significant deposition in the trachea and in more heterogeneous lung distribution. Our left intrabronchial instillation technique yielded a concentrated deposition into the left lung. We conclude that animal dosing techniques and devices result in varying patterns of particle deposition that will impact biokinetic and toxicity studies.

Introduction

The respiratory tract is a common route of entry for particles to enter the body and the most important for their translocation to various other organs. With the advent of nanotechnology, studies of the biological consequences and fate of nanoparticles using animal models are

[*]Corresponding Author: Ramon M. Molina, Molecular and Integrative Physiological Sciences Program, Department of Environmental Health, Harvard T.H. Chan School of Public Health, 665 Huntington Avenue, Boston, MA 02115, USA., Phone: 1-617-432-2311, Fax: 1-617-432-4710, rmolina@hsph.harvard.edu.

Declaration of interest

The authors declare no conflict of interests in this paper.

increasing. Inhaled particles have been shown to deposit variably between the upper and lower respiratory regions (Asgharian et al., 2014, Xi et al., 2014). Depending on particle size, shape, density, and hygroscopicity, inhaled particles deposit in different regions via different mechanisms, such as gravitational settling, impaction, and interception and diffusion (Brain and Valberg, 1979, Heyder, 1982, Brain et al., 2014). Detailed reviews of mechanisms of deposition of inhaled particles are available (Asgharian et al., 2014, Heyder, 2004, Londahl et al., 2014, Tsuda et al., 2013).

Studies examining biokinetics of nanoparticles and their adverse effects when introduced into the respiratory tract are essential. Dosing of nanoparticles directly into the respiratory tract of experimental animals can be achieved by aerosolization or insufflation of dry powders, by microspraying, or by intratracheal instillation of nanoparticle suspensions. When particles dispersed in a liquid suspension are introduced into the respiratory tract, gravity causes the particle-carrier fluid to reach dependent small airways and parenchyma where the carrier fluid is rapidly absorbed into the pulmonary circulation, leaving behind the particles on the internal surfaces of the lungs. Different dosing methods have advantages and disadvantages. Due to the relative lower ventilation rate of rodents compared to aerosol generator output, large amounts of material need to be aerosolized to achieve a desired deposited dose by inhalation for studying biokinetics and biologic effects. This is a major problem when dealing with expensive or toxic radiolabeled nanoparticles. In addition, pulmonary aerosol deposition rates, and hence initially deposited doses, vary among animals. Conversely, although intratracheal instillation is a less physiological means for particle delivery, it allows for precise dosing of particles into the lungs at a specified time. Pulmonary delivery of dry powder formulations for testing or therapeutic applications using insufflation technique has been of increased interest lately, as it allows for precise dosing of particles in their native dry form. However, this technique is influenced by the physico-chemical properties of the material and the method of dispersion with air. While instillation, insufflation and microspraying procedures have various advantages in terms of the ease with which precise doses can be introduced, their resulting particle distributions within the lungs are important to compare.

Several studies have examined the factors affecting pulmonary distribution of inhaled or instilled particles in animals. A previous study compared the distribution of radiolabeled ^{99m}Tc particles in the lungs of rats and hamsters after inhalation exposure versus instillation of particle suspension (Brain et al., 1976). They showed that animals receiving intratracheal instillations demonstrated less uniform distribution patterns with preferential deposition in the dependent portions of the lung. The aerosol groups showed more even distribution with preferential deposition in the apical lobes. With similar techniques, it has also been shown that certain lung diseases (Sweeney et al., 1987, Sweeney et al., 1983b, Sweeney et al., 1995), anesthesia (Sweeney et al., 1983a) and exercise (Sweeney et al., 1990) alter particle deposition and anatomic distribution of retained particles in animals inhaling radioactive aerosols. A previous study compared the lung distribution of neutron activated cerium oxide (CeO_2) administered by single intratracheal instillation with inhalation of aerosolized particle suspension (Pritchard et al., 1985). They found that inhalation exposure results in a more uniform particle distribution compared to instillation. Several studies have employed microspraying (Bivas-Benita et al., 2005, Tada et

al., 2013) and insufflation techniques (Hoppentocht et al., 2014, Morello et al., 2009) using commercially available Penn-Century (Wyndmoor, PA) devices. The generation of a plume of liquid aerosol is achieved with a high-pressure syringe and a special instillation tube that aerosolizes solutions or suspensions (Microsprayer® aerosolizer). Aerosolization of dry powder (insufflation) is achieved using an insufflator (Dry Powder Insufflator™). It is a hand-operated device that delivers a cloud of fine particles from the end of a delivery (instillation) tube.

In this study, we compare the distribution of neutron activated CeO_2 nanoparticles (NPs) in the lungs following administration by 1) single intratracheal instillation, 2) left intrabronchial instillation, 3) microspraying of nanoparticle suspension and 4) insufflation of dry nanoparticles. CeO_2 NPs were selected for our investigation since CeO_2 NPs are relatively insoluble and are cleared very slowly from the lungs (Geraets et al., 2012, He et al., 2010, Molina et al., 2014).

Materials and Methods

Animals

The Harvard Medical Area Animal Care and Use Committee approved the protocols in this study. Male Wistar Han rats (8 weeks old) were obtained from Charles River Laboratories (Wilmington, MA) and housed in standard microisolator cages under controlled conditions of temperature, humidity, and light at the Harvard Center for Comparative Medicine. They were fed commercial chow (PicoLab Rodent Diet 5053, Framingham, MA) and were provided with reverse-osmosis purified water *ad libitum*. The animals were acclimatized in the facility for 7 days prior to the start of experiments, at which time their mean weight was 268.8 ± 12.5 g.

Characterization of CeO_2 nanoparticles

The cerium oxide nanoparticles used in this study were obtained from Mercator GmbH (Berlin, Germany). These are a test material assigned the specific code NM-212 by the program for safety testing of manufactured nanomaterials sponsored by the Organization for Economic Cooperation and Development. Extensive characterization of CeO_2 NM-212 has been previously reported by the European Commission's Joint Research Centre (Singh et al., 2014). The sample used in this study was characterized based on nano-specific guidelines by the European Chemicals Agency (ECHA) (ECHA, 2012). Additional characterization of NM-212 by the authors of the present study has been published previously (Molina et al., 2014).

Neutron activation of CeO_2 nanoparticles

Cerium oxide nanoparticles were neutron activated at the MIT Nuclear Reactor Laboratory (Cambridge, MA) with a thermal neutron flux of 5×10^{13} n/cm^2/s for 24 hours. This process generated the radioisotope ^{141}Ce, which decays with a half-life of 32.5 days and emits gamma rays with an energy of 145.4 KeV. The specific activity of the resulting ^{141}Ce was 5.69 μCi per mg CeO_2.

Preparation of CeO_2 nanoparticle suspensions for animal dosing

Particle suspensions at 3.33 mg/ml concentration were prepared in sterile distilled water in conical polyethylene tubes. A critical dispersion sonication energy (DSE_{cr}) was used to achieve the smallest possible particle agglomerate size, as previously reported (Cohen et al., 2013). The suspensions were sonicated at 242 J/ml (20 min/ml at 0.2 watt power output) in a cup sonicator fitted on Sonifier S-450A (Branson Ultrasonics, Danbury, CT). The sample tubes were immersed in running cold water to minimize heating of the particles during sonication. The hydrodynamic diameter (H_D), polydispersity index (PdI), and zeta potential (ζ) of each suspension were measured by dynamic light scattering using a Zetasizer Nano-ZS (Malvern Instruments, Worcestershire, UK).

Intratracheal instillation

Prior to intratracheal instillation, the rats were anesthetized with vaporized isoflurane and weighed. The dose for each rat was adjusted to each body weight (5 mg/kg, 1.5 ml/kg). Each pre-measured sonicated nanoparticle suspension was loaded in a 1 ml sterile syringe attached to a 3″ 22G stainless steel Luer gavage needle with a 1.25mm ball tip (Cadence Science, Lake Success, NY). The anesthetized rat was placed on a slanted board (30° from vertical) in supine position and was supported by an elastic band under the upper incisors. The particle suspension was delivered to the lungs just above the tracheal bifurcation after the blunt gavage needle was inserted between the vocal cords and through the trachea. The larynx was transilluminated with a microscope lamp shining on the neck. The nanoparticle suspension was delivered in a bolus within 3 seconds. The instilled rat was left on the slanted board with its chest gently massaged while being allowed to recover from anesthesia.

Microsprayer instillation

Rats used for microspray instillation were similarly anesthetized and placed on the slanted board as described above. Microspray instillation was performed using a Penn-Century MicroSprayer® aerosolizer (Wyndmoor, PA). It is a patented air-free atomizer that works by manual pressure. There are tiny holes in the tip of the device that generate an aerosol when liquids, solutions or suspensions are pushed through them with sufficient speed and force. We used a 1 ml gas-tight polycarbonate syringe suitable for the pressure needed to operate the MicroSprayer® Aerosolizer – Model IA-1B. The same mass and volume dose of $^{141}CeO_2$ nanoparticles used for intratracheal instillation was employed. A pre-measured sonicated nanoparticle suspension was loaded in a 1 ml polycarbonate syringe (B-SYR, Penn-Century) attached to a MicroSprayer® aerosolizer (Model 1A-1B, Penn-Century). The nanoparticle suspension was delivered to the lungs just above the tracheal bifurcation with the MicroSprayer® aerosolizer inserted through the trachea as described earlier for IT instillation. The entire liquid bolus was aerosolized with a quick and forceful push of the plunger. As before, dosed rats were allowed to recover from anesthesia while remaining suspended on the slanted board.

Left intrabronchial instillation

Selective instillation of a smaller volume (10% of the IT dose, or 0.5mg/kg and 0.15 ml/kg) of the same $^{141}CeO_2$ nanoparticle suspension into the left lobe of the rat lung was achieved

with a 3″ 22G stainless steel Luer feeding needle with a 1.25mm ball tip (Cadence Science, Lake Success, NY) modified to introduce a 9° angle 8mm from its tip. This allows easier insertion into the left bronchus, and the low volume dose prevents spillover into the contralateral right lobes. The left-lung intralobar instillation was performed by inserting the modified needle into the oropharynx with the ball tip angled ventrally. Once past the glottis, the ball tip was rotated to the rat's left side and gently moved down and to the left to just beyond the bronchial bifurcation. The effect was to position the ball tip of the gavage needle within the left bronchus. The recovery and positioning of the dosed rats were as in the IT-instilled rats.

Insufflation

We used the Penn-Century Dry Powder Insufflator™ DP-4 (Penn-Century, Wyndmoor, PA) which is a hand-operated pulmonary delivery device. It is designed to produce a cloud of fine particles from the end of a small-diameter delivery tube. The body of the device is made of chemically resistant PEEK™ parts and silicone valves. The device is sterilizable and reusable. Insufflation of dry powder is achieved by a Penn-Century air pump (Model AP-1). It is designed to blow air through the loaded powder sample to create an aerosol for delivery. The pump has a spring-loaded thumb button that automatically returns. It permits the user to rapidly generate single pulses or puffs of air at a specific volume each time the thumb button is depressed. The device can be adjusted to administer pulses of air from 0–5 ml depending on the lung capacity or tidal volume of the animal to be dosed. The pump delivers the same air volume pulse each time. $^{141}CeO_2$ nanoparticles were insufflated with 10 pulses of 1.5 ml air volume. The mass dose was 5 mg/kg.

Size characterization of CeO_2 nanoparticle suspension and aerosol

The size distribution of the sonicated suspensions of nanoparticle agglomerates was determined by dynamic light scattering (DLS) using a Zetasizer Nano-ZS (Malvern Instruments, Worcestershire, UK). The size distribution of the dry powder aerosols generated by the Penn-Century Dry Powder Insufflator™ and the aerosols produced by the Penn-Century microsprayer were analyzed by scanning mobility particle sizer (SMPS; model 3080) and water-based condensation particle counter (WCPC; model 3085) (TSI, Inc., Shoreview, MN). Separate measurements of microsprayed and insufflated nanoceria aerosols were also performed using an Aerodynamic Particle Sizer (APS) spectrometer (Model 3321) (TSI, Inc., Shoreview, MN).

Experimental design

Forty-eight rats were divided into 4 groups. Groups of twelve rats each were assigned to intratracheal instillation, Penn-Century microspray instillation, left intralobar instillation or Penn-Century DP-4 insufflation. Six rats from each dosing group were analyzed at 5 min post-dosing while the other six rats were individually housed in a metabolism cage for fecal and urine sample collection with food and water *ad libitum*. Twenty-four hour samples were collected. At 5 min or 24 hr post-dosing, rats were humanely killed with isoflurane anesthesia followed by exsanguination via the abdominal aorta. After euthanasia, the whole lung, tracheobronchial lymph nodes, liver and the entire gastrointestinal tract were collected. All tissues except the lungs were placed in pre-weighed tubes. The weight of each sample

was recorded. Radioactivity was measured in a WIZARD Gamma Counter (PerkinElmer, Inc., Waltham, MA). Disintegrations per minute were calculated from the measured counts per minute (minus background) and the counter efficiency. All radioactivity data were adjusted for physical decay. Data were expressed as μCi/g and as a percentage of the administered dose retained in each organ or excreted in the urine and feces. The total radioactivity in the blood was estimated from measured aliquots and blood volume was calculated as 7% of the body weight (Brown et al., 1997, Schoeffner et al., 1999).

Each rat lung was carefully removed and cannulated with polyethylene tubing (PE-200) attached to a 16G needle. Then each lung was air-inflated at a constant 30 cm water pressure, and allowed to dry at room temperature for 4 days. Dried lung lobes were then carefully separated and sliced, as illustrated in Figure 1. Each lobe was subdivided into many pieces according to a scheme shown in Figure 1A. Each lung piece was placed in pre-weighed 15.7 × 65 mm polypropylene tube and its anatomical position and sample weight was recorded. The radioactivity of each piece was measured in a WIZARD Gamma Counter and data were expressed as μCi/mg of each piece. After correcting for radioactive decay of ^{141}Ce, the evenness index (El) of each lung piece was calculated as described earlier (Brain et al., 1976): EI =($\mu Ci/mg_{piece}$)/($\mu Ci/mg_{lung}$). If the nanoparticles were deposited uniformly throughout the lungs, all pieces would have an El of 1.0. An El < 1.0 means that a piece received less than its “share” of the radioactive nanoparticles and an El > 1.0 means that a piece received more than its “share.” The degree of departure from 1.0 among the pieces is a measure of the heterogeneity of the relative local nanoparticle retention. Evenness indices were compared among 1) lung pieces, 2) different lung lobes and 3) different regions from apex to the base of the lungs.

Statistical analysis

Means of distribution data on radioactivity in lungs and other organs were analyzed with multivariate analysis of variance (MANOVA) followed by Bonferroni (Dunn) *post hoc* tests using SAS Statistical Analysis Software (SAS Institute, Cary, NC). Frequency distributions of evenness indices were analyzed with Prism 5 (GraphPad Software, Inc., La Jolla, CA).

Results and Discussion

Nanoparticle characterization

The primary particle size of NM-212 nanoceria was 40 nm (Molina et al., 2014, Singh et al., 2014). We determined the particle size distribution of the nanoceria suspension used for the whole lung and left-lung intralobar instillation using dynamic light scattering. Nanoceria was suspended in deionized water at 3.33 mg/ml, sonicated at 242 J/ml and immediately analyzed in a Zetasizer Nano-ZS (Malvern Instruments, Worcestershire, UK). The size distribution is shown in Figure 2A. The average hydrodynamic diameter was approximately 106 ± 16 nm. The same nanoceria suspension was aerosolized using the Penn-Century MicroSprayer® Aerosolizer Model 1B into an enclosed chamber attached to an SMPS and WCPC. The aerosol size distribution is shown in Figure 2B after single microspraying. The mean mobility diameter size was 159 ± 5 nm (geometric mean 144 ± 6 nm) obtained from three separate measurements of microsprayed nanoceria suspension. The dry powder aerosol

generated by the Penn-Century Dry Powder Insufflator™ was similarly characterized using SMPS and WCPC. The device was loaded with 1.5 mg dry nanoceria and discharged four times with a Penn-Century air pump (Model AP-1) with a preset air volume of 1.5 ml. The size distribution at each discharge is shown in Figure 2C and Figure 2D. The count mean aerosol diameter (166 ± 3 nm) was calculated from measurements of four consecutive discharges. The particle concentration decreased with each discharge (Figure 2C). Based on this discharge profile, we set our insufflation protocol to 10 discharges to maximize delivery of the loaded nanoceria. To determine the size distribution of microsprayed and insufflated nanoceria above the 300 nm upper limit of the SMPS, we also measured the aerodynamic size using an APS spectrometer. Insufflated dry powder aerosol had higher count mean aerodynamic diameter (2.4 ± 0.13 micron) (geometric mean 2.1 ± 0.1 micron) (Figure 2F) than the microsprayed liquid aerosol (1.1 ± 0.11 micron) (geometric mean 0.88 ± 0.06 micron) (Figure 2E). The number particle concentrations of the larger size fractions in both microsprayed and insufflated nanoceria aerosols (Figures 2E and 2F) were lower than those of the smaller sized fractions (Figure 2B and 2C).

Fate of $^{141}CeO_2$ nanoparticles after liquid or microspray intratracheal instillation and dry powder insufflation

In order to compare the relative efficiency of particle delivery for each method, we measured the percentage of loaded radioactive nanoceria that remained in each delivery device. The syringe with attached gavage needle, Penn-Century MicroSprayer® Aerosolizer needle or Penn-Century DP-4 Dry Powder Insufflator™ were rinsed twenty times with distilled water to remove residual $^{141}CeO_2$ nanoparticles. All rinses were collected and analyzed for radioactivity. Figure 3A shows that the remaining radioactivity was only 1.1% in IT instillation and 4.5% with microspraying needles, respectively. After left intrabronchial instillation, 10.3% remained in syringe and needle. Since the volume dose for left intrabronchial instillation was 10-fold lower than for intratracheal instillation, a tenfold higher residual radioactivity in the former likely indicates comparable residual volumes in the near-identical devices used for these two techniques. In contrast, dry powder insufflation resulted in a significantly higher fraction of loaded radioactive nanoceria remaining in the device (22.9%) compared to the other delivery methods (Figure 3A).

We then determined the fate of the $^{141}CeO_2$ dose from each pulmonary delivery device. The distribution of the loaded $^{141}CeO_2$ immediately after dosing (5 minutes) is shown in Figure 3B. As expected, negligible radioactivity was detectable in the extrapulmonary organs that we examined, such as the gastrointestinal tract, liver, blood and tracheobronchial lymph nodes. Seventy-five percent (Insufflation) to 87% (IT instillation) was found in the lungs (combined 50 lung pieces). These data suggest that the efficiency of delivering the dose into the respiratory tract was similar among the liquid suspension delivery methods. Despite the higher fraction remaining in the Penn-Century DP-4, most of the discharged dose was efficiently deposited in the lungs for all devices.

We also determined whether the delivery method influenced the fate of deposited $^{141}CeO_2$ nanoparticles over a period of 24 hours. Particles deposited more centrally (in larger airways) are cleared faster. The ^{141}Ce distribution in the lungs, other organs, and excreta at

24 hours post-dosing are shown in Figure 3C. We found that 2.24% (IT instillation), 0.04% (microspray administration), 8.8% (left intrabronchial instillation) and 40.5% (insufflation) of administered dose were cleared from the lungs. In both left intrabronchial instillation and insufflation, the remaining radioactivity was detected in the other examined organs and was excreted in the feces (Figure 3C). The high clearance after insufflation suggests a greater initial deposition in the trachea and large airways. Figure 3D shows the distribution in the extrapulmonary organs that we analyzed. Very little radioactivity was detected in the blood, liver and tracheobronchial lymph nodes. Almost all the extrapulmonary fraction was in the gastrointestinal tract (stomach, small and large intestine and cecum), indicating ingestion of nanoceria cleared from the upper respiratory tract.

Lung distribution of $^{141}CeO_2$ nanoparticles after liquid or aerosol intratracheal instillation and dry powder insufflation

To examine the deposition pattern of radioactive nanoceria, we calculated the evenness index of individual lung pieces as described earlier. The relative frequency distribution of evenness indices immediately (5 min) after $^{141}CeO_2$ nanoparticle administration is shown in Figure 4. We found that the distribution of evenness indices after IT instillation (Figure 4A) and microspraying (Figure 4B) were narrower than those of the other two delivery methods. There were much wider ranges for left intrabronchial instillation (Figure 4C) and insufflation (Figure 4D). The coefficient of variation, a standard measure of dispersion of frequency distribution data, was 69%, 89%, 196% and 188% for IT instillation, microspraying, left intrabronchial instillation and insufflation, respectively. These data indicate that the heterogeneity of lung distribution after IT instillation and microspraying was similar. Insufflation resulted in more heterogeneous distribution, as did the left intrabronchial instillation. Insufflation resulted in more uneven particle distribution primarily due to greater tracheal and airway deposition. The heterogeneity after left intrabronchial instillation was due to both intentional left lung delivery and the low volume dose that leads to more central deposition (Kharasch et al., 1991). The distributions of evenness index at 24 hours were similar to those at 5 minutes (Figure 5).

To examine the differences in $^{141}CeO_2$ spatial nanoparticle deposition, we examined the data in two different ways. First, we compared relative deposition in different lobes of the lungs; second, we examined deposition depth in strata from the apex to the base. The lobar analysis of deposited $^{141}CeO_2$ nanoparticle is shown in Figure 6A. We found that tracheal deposition was highest with insufflation and lowest with IT instillation. The presence of ^{141}Ce in the GI tract and its excretion in the feces post-insufflation is consistent with mucociliary clearance of nanoceria deposited predominantly in the trachea (Figure 6A). As expected, the vast majority of delivered dose was retained in the left lobe with selective left-lung instillation (71%). The left lobe and right caudal lobe received more radioactivity that the other lobes. Within each lobe, we also calculated the evenness indices of the different lung pieces to determine the heterogeneity of $^{141}CeO_2$ nanoparticle distribution within each lobe. Table 1 shows the evenness index of lung pieces within each lobe at 5 minutes post-administration of nanoceria. Our data shows that microspray administration resulted in more uniform distribution among the 5 lung lobes, as indicated by less variability in evenness index across the different lobes and lowest coefficient of variation (15%). Again, as expected, a much

higher $^{141}CeO_2$ nanoparticle concentration in the left lobe was found after deliberate left intrabronchial instillation. There were wide variations in evenness indices after insufflation, with the trachea having almost twice as much radioactivity as the lung lobes.

The extent of apex-to-base differences for $^{141}CeO_2$ nanoparticle deposition was determined by measuring radioactivity in lung pieces corresponding to 10 apex-to-base sections as indicated in Figure 1B. The percentage of delivered dose retained from the apex down to the base of the lungs is shown in Figure 6B. The percentage of dose deposited in the trachea was highest after insufflation. In general, there was increasing deposition from the apex to around the middle (A–F), then decreasing toward the base (G–J) of the lungs. The exception was with dry powder insufflation delivery, where deposition generally increased from the apex to the base. In addition, we analyzed concentration of $^{141}CeO_2$ nanoparticles within lung pieces comprising each apex-to-base slice. The evenness indices of lung pieces within each sagittal section at 5 minutes post-dosing are shown in Table 2. Similar trends of increasing concentration from the apex to the middle (A–F), then decreasing toward the base (G–J) of the lungs were also seen in the evenness index after IT, microspray and left intrabronchial instillation. On the other hand, there was a tendency for increasing $^{141}CeO_2$ nanoparticle concentration from the apex to the base after insufflation.

Further studies with modifications in insufflation parameters are needed. Since multiple discharges are necessary to administer the loaded powder, there is a high probability that the aerosol gets deposited in the trachea and larynx when animals exhale. Improvements in synchronizing the insufflation with inhalation cycles and altering the air volume may improve the efficiency of pulmonary delivery during insufflation.

Conclusions

Our data showed that the pulmonary distribution of deposited nanoceria depends on the method of pulmonary administration. Dosing of rats with nanoceria suspension using either bolus or microspraying result in similar spatial distribution. Insufflation of dry nanoceria powder results in significant (over 40%) deposition in the trachea and in more heterogeneous distribution within the lungs. The greatest heterogeneity in distribution was from dry powder insufflation. We conclude that animal dosing techniques result in different extents and patterns of particle deposition that may impact the results of biokinetic and toxicity studies.

Acknowledgments

Funding Information

This study was supported by the National Institutes of Health grant ES000002, The Hoffman Program in Health and Chemicals and MannKind Corporation. H.H. received support from the Science Without Borders Program of Brazil administered by CAPES, the Brazilian Coordinating Office for the Advancement of Higher Education.

The authors thank Dr. Jiayuan Zhao for technical help and Melissa Curran for editorial assistance.

References

ASGHARIAN B, PRICE OT, OLDHAM M, CHEN LC, SAUNDERS EL, GORDON T, MIKHEEV VB, MINARD KR, TEEGUARDEN JG. Computational modeling of nanoscale and microscale

particle deposition, retention and dosimetry in the mouse respiratory tract. Inhal Toxicol. 2014; 26:829–42. [PubMed: 25373829]

BIVAS-BENITA M, ZWIER R, JUNGINGER HE, BORCHARD G. Non-invasive pulmonary aerosol delivery in mice by the endotracheal route. Eur J Pharm Biopharm. 2005; 61:214–8. [PubMed: 16039104]

BRAIN JD, KNUDSON DE, SOROKIN SP, DAVIS MA. Pulmonary distribution of particles given by intratracheal instillation or by aerosol inhalation. Environ Res. 1976; 11:13–33. [PubMed: 1253768]

BRAIN, JD.; KREYLING, WG.; GODLESKI, J. Inhalation Toxicology. In: HAYES, W.; KRUGER, CL., editors. Hayes' Principles and Methods of Toxicology. 6. Boca Raton: CRC Press; 2014.

BRAIN JD, VALBERG PA. Deposition of aerosol in the respiratory tract. Am Rev Respir Dis. 1979; 120:1325–73. [PubMed: 391112]

BROWN RP, DELP MD, LINDSTEDT SL, RHOMBERG LR, BELILES RP. Physiological parameter values for physiologically based pharmacokinetic models. Toxicol Ind Health. 1997; 13:407–84. [PubMed: 9249929]

COHEN J, DELOID G, PYRGIOTAKIS G, DEMOKRITOU P. Interactions of engineered nanomaterials in physiological media and implications for in vitro dosimetry. Nanotoxicology. 2013; 7:417–31. [PubMed: 22393878]

ECHA. Guidance on information requirements and chemical safety assessment: Appendix R7-1 Recommendations for nanomaterials applicable to Chapter R7a - Endpoint specific guidance - ECHA-12-G-03-EN. European Chemicals Agency; 2012. (European Chemicals Agency)

GERAETS L, OOMEN AG, SCHROETER JD, COLEMAN VA, CASSEE FR. Tissue distribution of inhaled micro- and nano-sized cerium oxide particles in rats: results from a 28-day exposure study. Toxicol Sci. 2012; 127:463–73. [PubMed: 22430073]

HE X, ZHANG H, MA Y, BAI W, ZHANG Z, LU K, DING Y, ZHAO Y, CHAI Z. Lung deposition and extrapulmonary translocation of nano-ceria after intratracheal instillation. Nanotechnology. 2010; 21:285103. [PubMed: 20562477]

HEYDER J. Particle transport onto human airway surfaces. Eur J Respir Dis Suppl. 1982; 119:29–50. [PubMed: 6954086]

HEYDER J. Deposition of inhaled particles in the human respiratory tract and consequences for regional targeting in respiratory drug delivery. Proc Am Thorac Soc. 2004; 1:315–20. [PubMed: 16113452]

HOPPENTOCHT M, HOSTE C, HAGEDOORN P, FRIJLINK HW, DE BOER AH. In vitro evaluation of the DP-4M PennCentury insufflator. Eur J Pharm Biopharm. 2014; 88:153–9. [PubMed: 24993307]

KHARASCH VS, SWEENEY TD, FREDBERG J, LEHR J, DAMOKOSH AI, AVERY ME, BRAIN JD. Pulmonary surfactant as a vehicle for intratracheal delivery of technetium sulfur colloid and pentamidine in hamster lungs. Am Rev Respir Dis. 1991; 144:909–13. [PubMed: 1928969]

LONDAHL J, MOLLER W, PAGELS JH, KREYLING WG, SWIETLICKI E, SCHMID O. Measurement techniques for respiratory tract deposition of airborne nanoparticles: a critical review. J Aerosol Med Pulm Drug Deliv. 2014; 27:229–54. [PubMed: 24151837]

MOLINA RM, KONDURU NV, JIMENEZ RJ, PYRGIOTAKIS G, DEMOKRITOU P, WOHLLEBEN W, BRAIN JD. Bioavailability, distribution and clearance of tracheally instilled, gavaged or injected cerium dioxide nanoparticles and ionic cerium. Environ Sci:Nano. 2014; 1:561–573.

MORELLO M, KRONE CL, DICKERSON S, HOWERTH E, GERMISHUIZEN WA, WONG YL, EDWARDS D, BLOOM BR, HONDALUS MK. Dry-powder pulmonary insufflation in the mouse for application to vaccine or drug studies. Tuberculosis (Edinb). 2009; 89:371–7. [PubMed: 19632897]

PRITCHARD JN, HOLMES A, EVANS JC, EVANS N, EVANS RJ, MORGAN A. The distribution of dust in the rat lung following administration by inhalation and by single intratracheal instillation. Environ Res. 1985; 36:268–97. [PubMed: 3979359]

SCHOEFFNER DJ, WARREN DA, MURALIDARA S, BRUCKNER JV, SIMMONS JE. Organ weights and fat volume in rats as a function of strain and age. J Toxicol Environ Health A. 1999; 56:449–62. [PubMed: 10201633]

SINGH, C.; FRIEDRICHS, S.; CECCONE, G.; GIBSON, N.; JENSEN, KA.; LEVIN, M.; INFANTE, HG.; CARLANDER, D.; RASMUSSEN, K. JRC Repository: NM-series of Representative Manufactured Nanomaterials. Ispra, Italy: European Commission Joint Research Centre Institute for Health and Consumer Protection; 2014. Cerium Dioxide, NM-211, NM-212, NM-213. Characterisation and test item preparation.

SWEENEY TD, BRAIN JD, LEAVITT SA, GODLESKI JJ. Emphysema alters the deposition pattern of inhaled particles in hamsters. Am J Pathol. 1987; 128:19–28. [PubMed: 3649192]

SWEENEY TD, BRAIN JD, LEMOTT S. Anesthesia alters the pattern of aerosol retention in hamsters. J Appl Physiol Respir Environ Exerc Physiol. 1983a; 54:37–44. [PubMed: 6826421]

SWEENEY TD, BRAIN JD, TRYKA AF, GODLESKI JJ. Retention of inhaled particles in hamsters with pulmonary fibrosis. Am Rev Respir Dis. 1983b; 128:138–43. [PubMed: 6191603]

SWEENEY TD, SKORNIK WA, BRAIN JD, HATCH V, GODLESKI JJ. Chronic bronchitis alters the pattern of aerosol deposition in the lung. Am J Respir Crit Care Med. 1995; 151:482–8. [PubMed: 7842210]

SWEENEY TD, TRYKA AF, BRAIN JD. Effect of exercise on redistribution and clearance of inhaled particles from hamster lungs. J Appl Physiol (1985). 1990; 68:967–72. [PubMed: 2341362]

TADA Y, YANO N, TAKAHASHI H, YUZAWA K, ANDO H, KUBO Y, NAGASAWA A, INOMATA A, OGATA A, NAKAE D. Long-term Pulmonary Responses to Quadweekly Intermittent Intratracheal Spray Instillations of Magnetite (Fe3O4) Nanoparticles for 52 Weeks in Fischer 344 Rats. J Toxicol Pathol. 2013; 26:393–403. [PubMed: 24526812]

TSUDA A, HENRY FS, BUTLER JP. Particle transport and deposition: basic physics of particle kinetics. Compr Physiol. 2013; 3:1437–71. [PubMed: 24265235]

XI J, SI XA, KIM J, MCKEE E, LIN EB. Exhaled aerosol pattern discloses lung structural abnormality: a sensitivity study using computational modeling and fractal analysis. PLoS One. 2014; 9:e104682. [PubMed: 25105680]

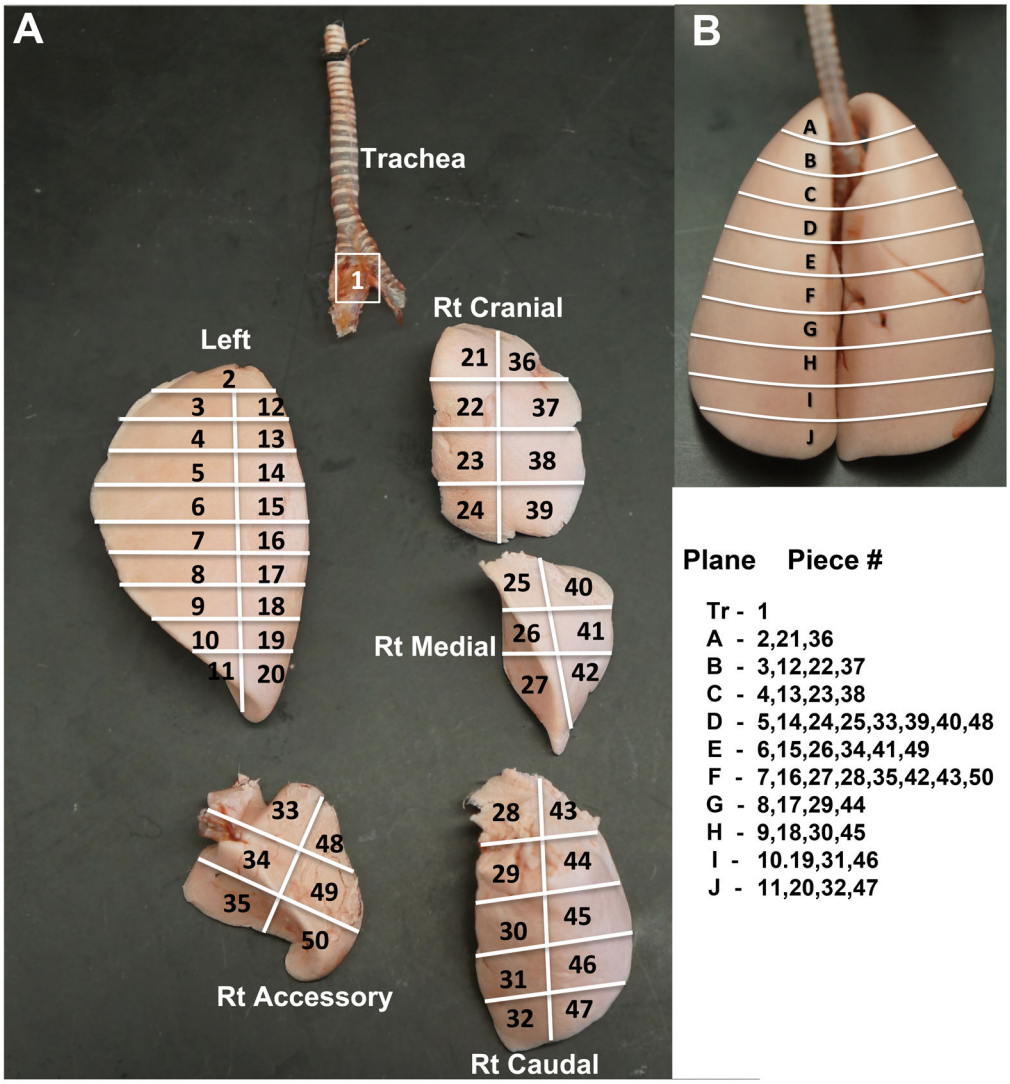

Figure 1.

(**A)** Systematized slicing of dried lungs. The trachea and bronchi, left lung, right cranial, medial, caudal and accessory lobes were carefully separated. Each lobe was uniformly sliced according the scheme shown. The orientation of the 4 right lobes reflects their position in the dried lung (**B).** Dorsal view of dried rat lung. The lines indicate the approximate sections (A to J) from the apex to the base of the lung. The lung pieces from each lung lobe corresponding to each apex-to-base section (plane) are shown.

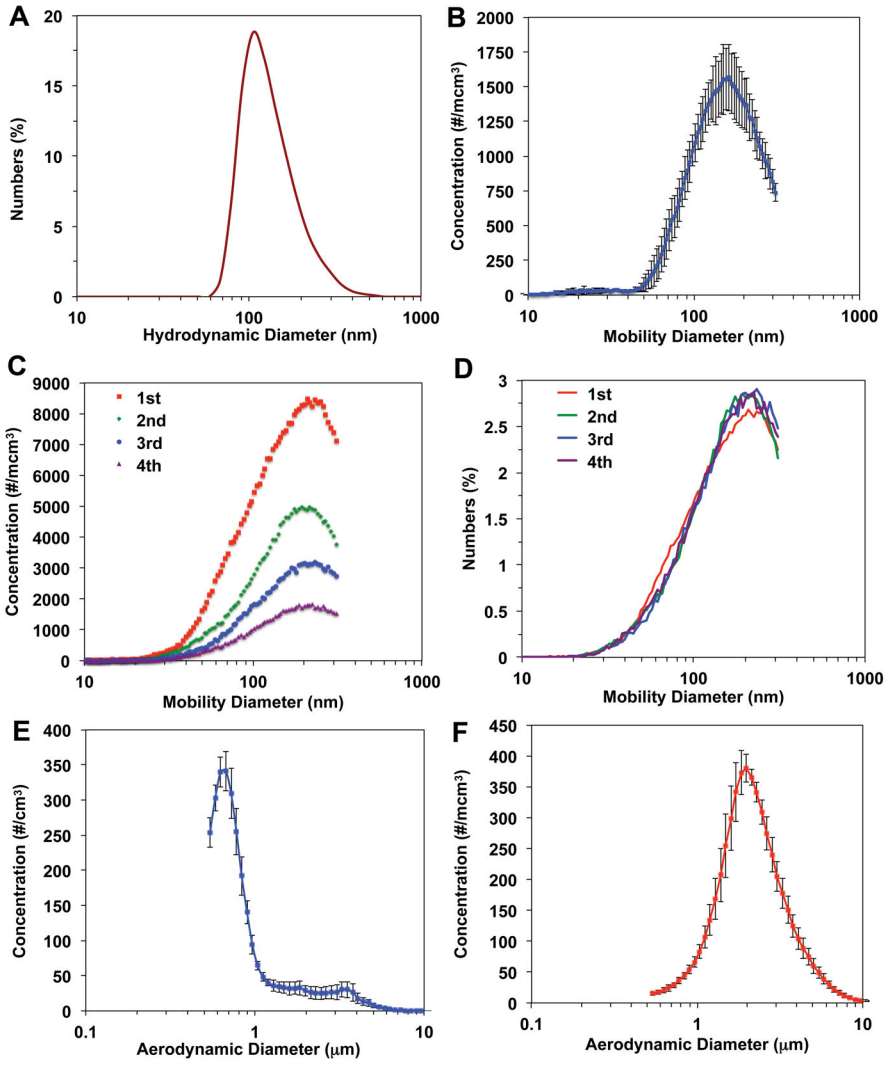

Figure 2.

Particle size distribution of nanoceria used in different delivery methods. (**A**) An aqueous suspension at 3.33 mg/ml in distilled water was dispersed with 242 J/ml sonication energy. The hydrodynamic diameter was immediately analyzed. This suspension was used for both IT and left intrabronchial instillation. (**B**) The same sonicated suspension was microsprayed using a Penn-Century Microsprayer aerosolizer into a 2-inch cylindrical chamber. The aerosol size distribution was immediately measured by SMPS and WCPC. (**C**) The aerosol generated by Penn-Century DP-4 insufflator was also analyzed using SMPS and WCPC. The size distributions of the first 4 of 10 discharges are shown in particle number concentration per cubic cm. Although the particle concentrations decreased in subsequent discharges, the normalized size distributions among discharges were similar as shown in **D**. The mean count aerosol size distribution of microsprayed nanoceria suspension (n=3 measurements) and of insufflated dry powder (n=4 measurements) analyzed with Aerodynamic Particle Sizer (APS) spectrometer are shown in **E** and **F**, respectively.

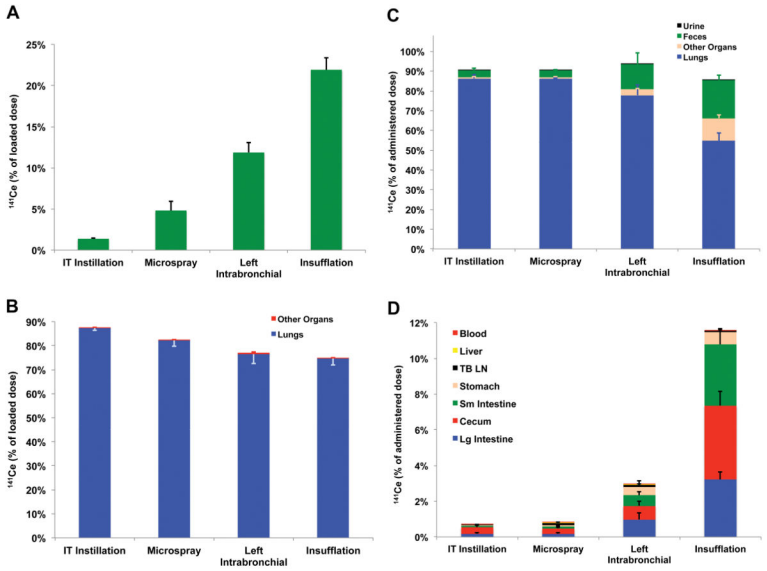

Figure 3.

Distribution of $^{141}CeO_2$ nanoparticles after 4 methods of pulmonary administration in rats. (**A)** The amount of ^{141}Ce remaining in each dosing device after dose delivery is shown as percentage of loaded dose. The remnant radioactivity was lowest in the IT instillation needle-syringe combination (1.3%) and highest in the insufflator (24.2%). (**B**) Distribution of the discharged $^{141}CeO_2$ nanoparticles dose. Nearly the entire radioactivity was measured in the 50 lung pieces. There is an inverse relationship between A and B. (**C)** Organ distribution of administered ^{141}Ce dose at 24 hours post-dosing. The fraction of administered dose remaining in the lungs was similar after IT and microspray instillation and lowest after insufflation. Most of the radioactivity was in the feces and in the other organs examined. The majority of recovered ^{141}Ce in the other organs was found in the stomach, small and large intestine and cecum (**D**). Data are mean ± SE % of dose, n= 6 rats/ group.

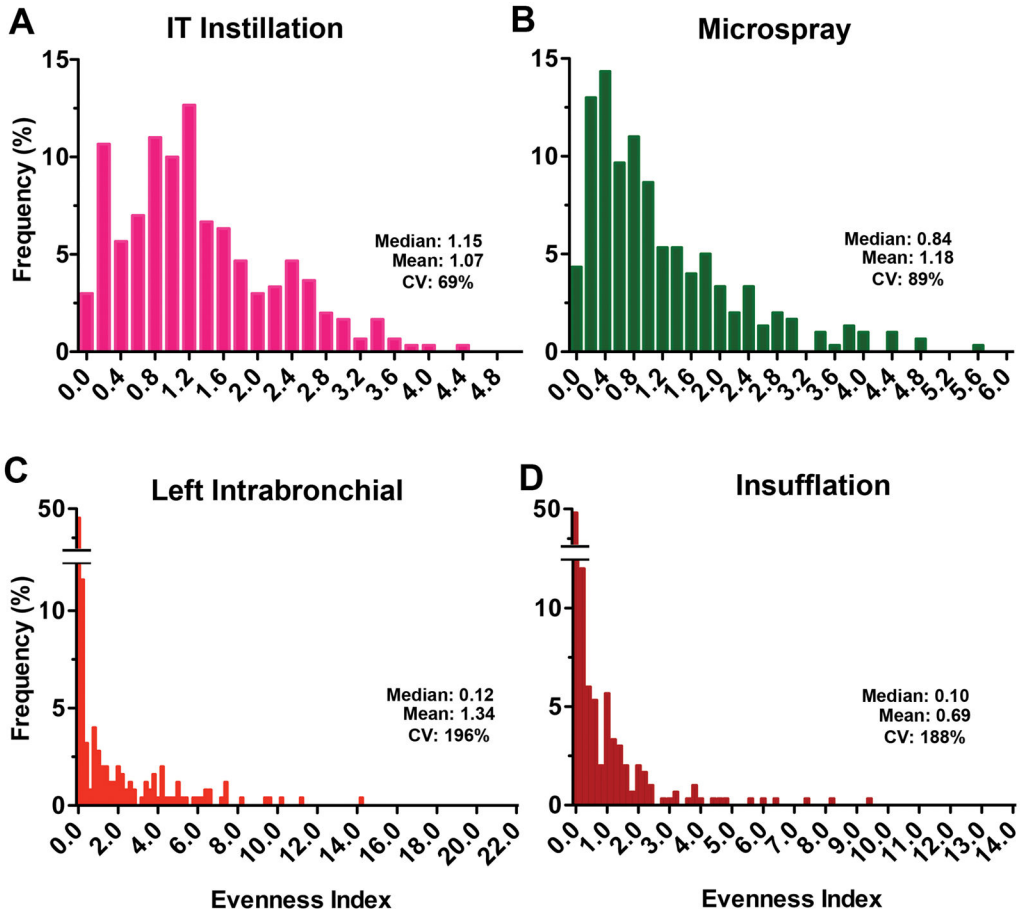

Figure 4.

Relative frequency distribution of evenness indices at 5 minutes after administration of $^{141}CeO_2$ nanoparticles. The evenness index of each lung piece from 6 rats/group was determined and the overall evenness index distribution is shown for bolus IT instillation (**A**), microspray instillation (**B**), left intrabronchial instillation (**C**) and insufflation (**D**). Data are relative frequency of evenness indices of 300 lung pieces (50 pieces/rat, 6 rats/group). The x axes show the inclusive lower limit of each bar.

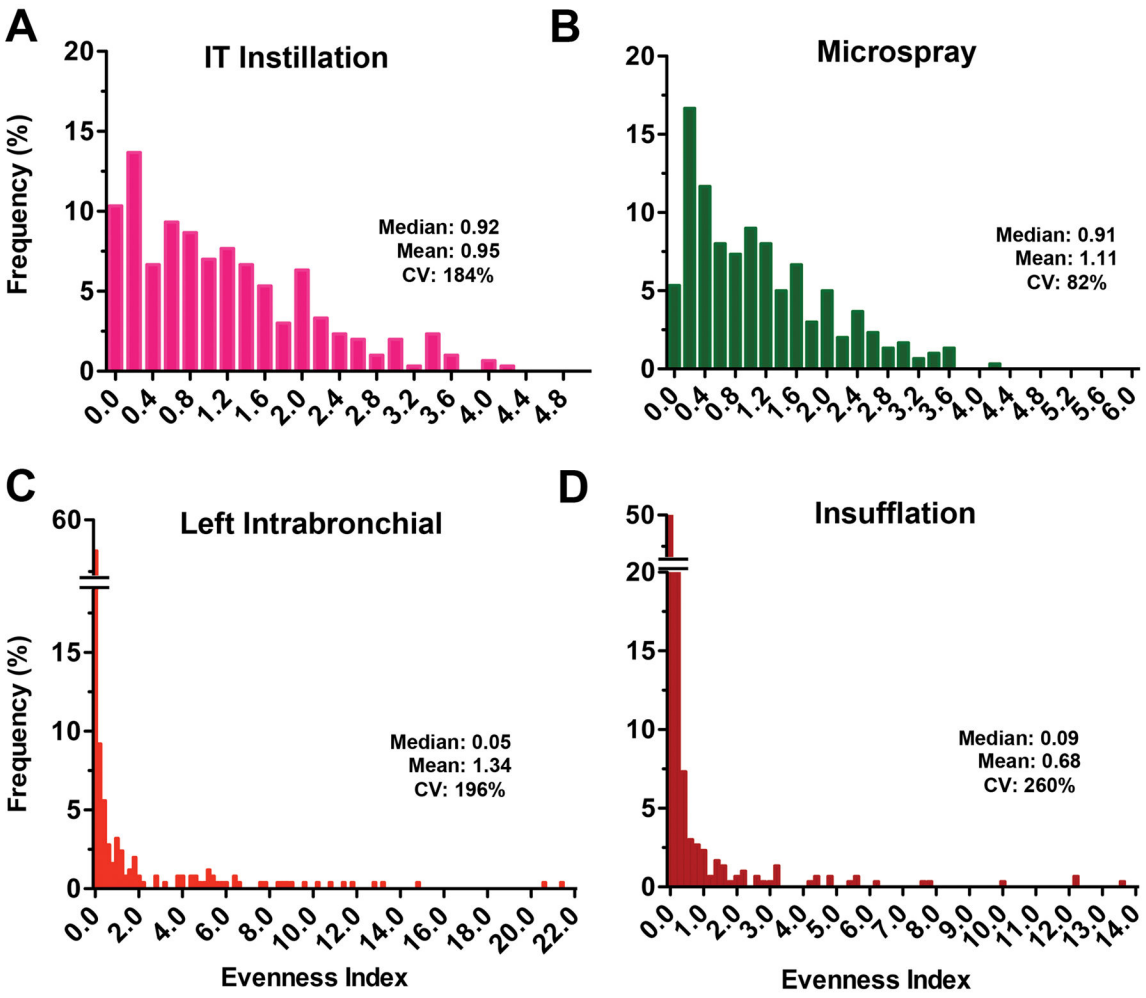

Figure 5.

Relative frequency distribution of evenness indices at 24 hours after administration of $^{141}CeO_2$ nanoparticles. The evenness index of each lung piece from 6 rats/group was determined and the overall evenness index distribution is shown for IT instillation (**A**), microspray instillation (**B**), left intrabronchial instillation (**C**) and insufflation (**D**). Data are relative frequency of evenness indices of 300 lung pieces (50 pieces/rat, 6 rats/group). The x axes show the inclusive lower limit of each bar.

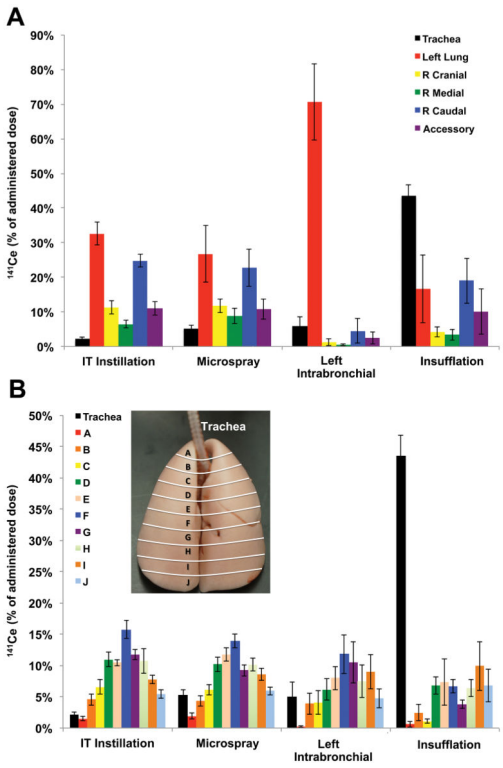

Figure 6.

Pulmonary distribution of $^{141}CeO_2$ nanoparticles at 5 minutes post-dosing. (**A**) Distribution of $^{141}CeO_2$ nanoparticles in different lung lobes and the trachea. (**B**) Distribution of delivered dose corresponding to 10 apex-to-base sections (trachea was not included in the analysis, inset). Data are mean ± SE % of dose, n= 6 rats/group.

Table 1

Evenness index of lung pieces at 5 minutes post-dosing from each lung lobe of rats dosed with $^{141}CeO_2$ nanoparticles.

Lung lobe	IT Instillation	Microspray	Left Intrabronchial	Insufflation
	Mean ± SE	Mean ± SE	Mean ± SE	Mean ± SE
Trachea	0.09 ± 0.02	0.27 ± 0.03	0.36 ± 0.18	1.91 ± 0.17
Left	1.50 ± 0.14	1.24 ± 0.41	3.07 ± 0.48	0.70 ± 0.41
Right cranial	0.85 ± 0.13	1.49 ± 0.18	0.14 ± 0.10	0.44 ± 0.15
Right medial	0.58 ± 0.08	0.97 ± 0.18	0.03 ± 0.01	0.31 ± 0.14
Right caudal	0.96 ± 0.09	1.29 ± 0.25	0.34 ± 0.29	1.17 ± 0.35
Right Accessory	1.00 ± 0.16	1.25 ± 0.27	0.32 ± 0.23	0.95 ± 0.58
All lobes	0.98 ± 0.15	1.25 ± 0.08	0.78 ± 0.58	0.71 ± 0.16
Coefficient of variation	34%	15%	166%	49%

Data are mean ± SE of EI in each lung lobe and trachea, n=6 rats/group.

Table 2

Evenness index of lung pieces at 5 minutes post-dosing from the apex to the base of rat lungs dosed with $^{141}CeO_2$ nanoparticles using different techniques.

Apex-to-base section	IT Instillation	Microspray	Left Intrabronchial	Insufflation
	Mean ± SE	Mean ± SE	Mean ± SE	Mean ± SE
A	0.38 ± 0.06	0.90 ± 0.21	0.17 ± 0.09	0.20 ± 0.13
B	0.92 ± 0.17	1.26 ± 0.12	1.21 ± 0.50	0.51 ± 0.26
C	1.22 ± 0.23	1.58 ± 0.23	0.89 ± 0.30	0.24 ± 0.10
D	0.84 ± 0.05	1.00 ± 0.12	1.15 ± 0.30	0.49 ± 0.09
E	1.09 ± 0.07	1.36 ± 0.14	1.82 ± 0.28	0.78 ± 0.36
F	1.04 ± 0.07	1.31 ± 0.09	2.84 ± 0.54	0.68 ± 0.11
G	1.44 ± 0.11	1.47 ± 0.07	2.05 ± 0.41	0.69 ± 0.13
H	1.37 ± 0.21	1.55 ± 0.15	1.69 ± 0.47	0.87 ± 0.18
I	1.14 ± 0.15	1.22 ± 0.12	1.75 ± 0.33	1.47 ± 0.49
J	0.77 ± 0.18	0.81 ± 0.15	1.75± 0.19	1.43 ± 0.45
All sections	1.02 ± 0.10	1.25 ± 0.08	1.41 ± 0.24	0.74 ± 0.14
Coefficient of variation	31%	22%	55%	59%

Data are mean ± SE of EI in each apex-to-base section, n=6 rats/group. Evenness indices in the left intrabronchial group were based on lung slices in the left lung lobe only.